SEPARATED LAMINAR BOUNDARY LAYERS

Odus R. Burggraf
The Ohio State University

SUMMARY

Classical boundary-layer theory is inadequate to deal with the problem of flow separation owing to its underlying assumption that the boundary layer has an insignificant effect on the external stream. This difficulty is resolved by the modern theory which includes interaction with the external flow. This newer theory is described from the viewpoint of the asymptotic triple-deck structure. Several triple-deck studies are reviewed with emphasis on results of interest in aeronautical applications.

INTRODUCTION

Separated flow occurs when an attached boundary layer encounters a downstream compressive disturbance of sufficient magnitude. Observations show that the separation point lies at a rather long distance upstream of the disturbance, contradicting the inherent nature of Prandtl's boundary layer theory that no upstream influence can occur. Crocco and Lees (ref. 1) have shown that coupling the pressure of the external inviscid flow to the displacement thickness of the boundary layer permits upstream influence to be consistent with the boundary-layer equations. This concept led to the integral methods of Lees and Reeves (ref. 2), and others, for viscous interacting flows. However, the correct mathematical structure of such flows was not given until the papers of Stewartson and Williams (ref. 3) and of Neiland (ref. 4) on self-induced separation in supersonic flows at high Reynolds number. Independently, the same asymptotic structure was shown to hold for incompressible flow at the trailing edge of an airfoil by Stewartson (ref. 5) and by Messiter (ref. 6). This flow structure, which Stewartson has named "the triple deck", has been found to be relevant in a wide variety of applications. The purpose of this paper is to review several of these triple-deck studies that are of interest in aeronautical applications.

THE TRIPLE DECK

A schematic of the triple-deck structure is shown in figure 1.

The parameter $\varepsilon = Re^{-1/8}$ (Re - Reynolds number) has been standardized in the theory because of the occurrence of various integer powers of ε. As indicated in the figure, the streamwise extent of the triple deck is of order ε^3, while the thicknesses of the lower, main, and upper decks are of order ε^5, ε^4, and ε^3, respectively. The dominant physical processes for large Re in each of the decks are as follows:

(1) The main deck is the continuation of the upstream boundary layer. It is essentially inviscid because of the short length (ε^3) of the interaction region. A slip velocity is produced at the base of the main deck by the pressure interaction.

(2) The lower deck is a viscous sublayer in which the slip velocity at the base of the main deck is reduced to zero at the wall. Because it is thin, the lower deck flow is governed by the boundary-layer equations. However, the condition of matching to the upper deck provides an unconventional boundary condition on these equations.

(3) The upper deck is a subregion of the outer potential flow where the pressure adjusts to the streamline displacement produced by the viscous flow below, thus completing the interaction process. For supersonic flow, the upper deck equations of motion reduce to the classical wave equation with simple-wave solutions. For subsonic flow, Laplace's equation results, with the usual Hilbert integrals governing the interaction between pressure and displacement thickness. In either subsonic or supersonic flow, upstream influence is permitted by the interaction process.

The mathematical details of triple-deck theory can be found in references 3 through 6; we shall concentrate here on some results of the theory.

COMPRESSION-RAMP STUDIES

Supersonic flow past a compression corner is a fundamental problem in aerodynamics. The inviscid flow is especially simple, with two uniform flow states divided by an oblique shock wave originating at the corner. The classical boundary-layer problem, however, has no solution since the upstream boundary layer is terminated by the infinitely adverse pressure gradient associated with the corner. Experimental observations show that the actual pressure rise does not occur discontinuously as inviscid theory predicts, but instead is smeared out over some interaction distance, with boundary-layer separation occurring ahead of the corner. This problem is natural for triple-deck theory, and solutions taken from references 7 and 8 are shown in figure 2. Here P, X, and α are scaled variables representing the pressure p^*, distance from the corner x^*, and ramp angle α^*:

$$p^* = p_\infty^* + \rho_\infty^* u_\infty^{*2} Re^{-1/4} C^{1/4} \lambda^{1/2} (M_\infty^2 - 1)^{-1/4} P(X)$$

$$x^*/L = Re^{-3/8} C^{3/8} \lambda^{-5/4} (M_\infty^2 - 1)^{-3/8} (T_W/T_\infty)^{3/2} X$$

$$\alpha^* = Re^{-1/4} C^{1/4} \lambda^{1/2} (M_\infty^2 \; 1)^{1/4} \alpha$$

The Reynolds number Re is based on conditions in the undisturbed inviscid flow ahead of the ramp (indicated by subscript ∞) and on the length L from leading edge to corner. C denotes the Chapman-Rubesin constant and λ is the Blasius constant (0.33206). ρ, u, T, and M are the usual symbols for density, velocity, temperature and Mach number.

The results of figure 2 show a smooth monotonically rising wall pressure for α below the value for incipient separation, $\alpha_i = 1.57$. (Note that classical theory would predict separation for any $\alpha^* > 0$). For α increasing above α_i, an inflection point appears and rapidly forms the pressure plateau observed in many experiments. The plateau pressure level is in close agreement with Williams value $P = 1.8$ for self-induced separation (ref. 9), corresponding to an obstacle far downstream of separation. In figure 2, the initial pressure distribution up to the plateau level is pushed upstream with invariant shape as α increases. This portion of the pressure distribution reproduces Williams' free-interaction solution, suggesting that as $\alpha \to \infty$ (α^* increasing beyond the $Re^{-1/4}$ scale) the separation point is pushed upstream to infinity (the interaction length exceeds the $Re^{-3/8}$ scale). In turn, this suggests that for large α(α^* beyond the $Re^{-1/4}$ scale), the separation region up to the plateau is still contained in the triple-deck structure, but that the constant pressure plateau and subsequent reattachment region develop on different scales.

An analysis of the flow structure based on these ideas is given in reference 10. The principal results are as follows. For ramp angle α^* of order one, the separation bubble is long, of the order of the distance L from leading edge to corner in length. The reattachment process is short, however, with length of the order of the boundary-layer thickness (i.e., of order $Re^{-1/2}$). Because of its small scale, reattachment is predominantly inviscid in nature, much as hypothesized by Chapman (ref. 11). Hence, the asymptotic analysis for large Reynolds number reveals the separating-reattaching flow to be three coupled but distinct regions: the separation region with length $O(L\ Re^{-3/8})$, in which the pressure rises to the plateau level ($P = 1.8$); the plateau region of constant pressure with length $O(L)$; and the reattachment region with length $O(L\ Re^{-1/2})$, in which the pressure rises from the plateau level to its final value with mainstream parallel to the ramp.

Figure 3 illustrates results of computations based on the above asymptotic theory. The experimental data are taken from reference 12. The flow conditions were $M_\infty = 2.55$, $Re_\infty = 200{,}000$ based on the distance L from leading edge to corner. This comparison shows that the pressure levels predicted by the theory are very good, although the initiation of the pressure rise is predicted somewhat early. For comparison, it may be noted that momentum-integral interaction theories exhibit a similar uncertainty in the point of initiation of the pressure rise, which is usually chosen to best agree with experiment. A similar adjustment of the theory could be made in figure 3 by means of an arbitrary origin shift in the asymptotic formulas.

A composite theory for finite Reynolds number is provided by the compressible boundary-layer equations coupled with a pressure-displacement condition. This set of equations includes all the terms from the Navier-Stokes equations that are included in the governing equations for each of the three regions identified by the asymptotic theory. A finite-difference algorithm of these interacting boundary-layer equations has been programmed by Werle and Vatsa (ref. 13). Their experience has shown that at high Reynolds numbers, accurate solutions can be obtained only by choosing the mesh size smaller than the length scales given by triple-deck theory, and in that case, the interacting boundary-layer solutions asymptote the triple-deck results for very large Reynolds numbers (ref. 8). As indicated in figure 4, at lower Reynolds numbers of practical interest, the interacting boundary-layer solutions agree quite well with both experimental data (ref. 14) and with solutions of the Navier-Stokes equations (ref. 15). The flow conditions were adiabatic with $M_\infty = 4$, $Re_\infty = 68{,}000$ based on distance to the corner. The presence of the plateau "kink", present in both the experimental data and Navier-Stokes solutions, but not evident in the interacting boundary-layer results, is caused by the sharp corner which was slightly rounded in the modelling of Werle and Vatsa. Otherwise the agreement is excellent, and it can be concluded that the interacting boundary-layer theory models weakly separated flows with accuracy satisfactory for engineering purposes. It should be noted, however, that the asymptotic theory indicates that normal pressure gradients, not present in the boundary-layer model, become important near reattachment when the separation bubble is large.

TRAILING EDGE STUDIES

Another area of importance in aerodynamics is the problem of viscous interaction at a trailing edge. The sudden change-over from the no-slip condition on the airfoil surface to the wake-continuity condition produces a significant viscous modification to the flow near the trailing edge, even for a flat plate at zero incidence. For the airfoil at incidence, lift is reduced due to viscous alteration of the Kutta condition. For unsteady motion, viscous phase effects may alter flutter boundaries. All these problems have been treated using triple-deck theory.

A schematic of the triple-deck structure is given in figure 5 for the case of an airfoil at zero incidence. The triple deck on the upper surface is reflected symmetrically below the airfoil. In classical boundary-layer theory, the viscous correction to the potential flow would produce a singularity in the pressure at the trailing edge, owing to the singular slope of the displacement thickness produced by the abrupt change of viscous boundary condition at the trailing edge. The coupling of pressure and displacement in the viscous-interaction theory eliminates this singularity. The fundamental trailing-edge problem of the flat plate at zero incidence has been solved independently by Jobe and Burggraf (ref. 16), by Veldman and van de Vooren (ref. 17), and by Melnik and Chow (ref. 18), all for incompressible flow. In addition, the same problem for supersonic flow has been treated by Daniels (ref. 19). A summary of the results is presented in figure 6, taken from reference 16. Here X is the triple-deck scaled-longitudinal coordinate, with X = 0 taken at the trailing edge, and P is the scaled pressure, both defined as before but with the Mach number factor, temperature ratio and Chapman-Rubesin constant deleted. A is a scaled (negative) displacement thickness, proportional to $Re^{-5/8}$.

The principal results indicated in figure 6 are the pressure fall as the flow is accelerated toward the trailing edge, and the accompanying rise of skin friction to a trailing-edge value nearly 35% greater than the Blasius value. Downstream of the trailing edge, the rapidly rising pressure overshoots the freestream value (P = 0) and then slowly decays for large X. The theoretical drag coefficient, also given in figure 6, compares amazingly well with both experimental data ($10 \le Re \le 10{,}000$), with RMS error of 3.5 percent over the range of the experimental data, and an error of 8 percent at Re = 1 and only 2 percent at Re = 15 when compared with the Navier-Stokes solutions.

The theoretical wake-velocity profile (ref. 18) is compared with experimental data (ref. 20) in figure 7. The centerline value predicted by Goldstein's non-interacting theory is shown for comparison. Transition to turbulence was observed to begin at a station coinciding with the maximum of the induced pressure, indicated in the figure, suggesting that viscous interaction may be important in predicting transition in wakes.

The case of an airfoil at angle of attack is more difficult to treat, as the upper and lower triple decks are no longer symmetrical. This problem has been solved for the supersonic case by Daniels (ref. 21), and very recently for the incompressible case by Chow and Melnick (ref. 22; see also ref. 18 for preliminary results). The flow structure is indicated in figure 8, which is now generalized to include the Stokes layers II_2 and III_2, which occur in the unsteady case only. For the steady case, regions II_1 and III_1 coincide and represent the conventional boundary layer; IV_1, IV_2, and IV_3 represent the triple deck, and regions V_1 and V_2 are the outer and inner layers of the wake as deduced by Goldstein. Viscous interaction occurs only in the triple deck, of course. Chow and Melnik carried out the flat-plate triple-deck solution for a range of angles-of-attack up to a value very near the stall limit α_S, which was estimated by extrapolating their solutions to zero shear stress on the upper surface. Below stall, the point of minimum shear stress occurs ahead of the trailing edge, but approaches the trailing edge in the stall limit. The reduction in lift coefficient due to viscous interaction is shown in figure 9. Chow and Melnik conclude that the stall is catastrophic, with $\Delta C_L \, Re^{-3/8} \to \infty$ in the double limit $Re \to \infty$, $\alpha \to \alpha_S$. However, this point is not yet definitely resolved.

The viscous flow about the trailing edge of a rapidly oscillating plate has been studied by Brown and Daniels (ref. 23). They find that to have an unsteady contribution of viscous interaction to the potential flow, the oscillation frequency, in either pitching or plunging motion, must satisfy $S = \omega^* L / u^*_\infty = O(Re^{1/4})$ where L is the plate length. For S large, even on this scale, there results two contributions to the unsteady lift having phase leads of 45° and 90°, with similar results for the moment. Further details of the analysis may be found in reference 23.

CONCLUDING REMARKS

The examples of viscous interaction theory summarized above should give the reader some idea of the contributions being made by modern boundary-layer theory that were not possible in classical theory. Many other examples could be given, such as leading edge separation bubbles, mass injection effects, swept configurations, and more, but space does not permit further discussion here. It is hoped that the reader has gained some appreciation for the potential of this rapidly expanding field of study.

REFERENCES

1. Crocco, L., and Lees, L.: J. Aero. Sci., Vol. 19, 1952, p. 649.

2. Lees, L., and Reeves, B.: AIAA J., Vol. 2, 1964, p. 1907.

3. Stewartson, K., and Williams, P. G.: Proc. Roy. Soc. A, Vol. 312, 1969, pp. 181-206.

4. Neiland, V.: Izv. Akad. Nauk SSSR, Mekh. Zhidk. Gaza, No. 4, 1969, p. 40.

5. Stewartson, K.: Mathematika, Vol. 16, 1969, p. 106.

6. Messiter, A. F.: SIAM J. Appl. Math., Vol. 18, 1970, p. 241.

7. Jenson, R., Burggraf, O. R., and Rizzetta, D.: Proc. 4th Int. Conf. on Numerical Methods in Fluid Dynamics, Lecture Notes in Physics, Vol 35, Springer-Verlag, 1975, p. 218.

8. Rizzetta, D.: Asymptotic Solution for Two-Dimensional Viscous Supersonic and Hypersonic Flows past Compression and Expansion Corners, Ph.D. Dissertation, Ohio State Univ., June 1976.

9. Williams, P. G.: Proc. 4th Int. Conf. on Numerical Methods in Fluid Dynamics, Lecture Notes in Physics, Vol. 35, Springer-Verlag, 1975, p. 445.

10. Burggraf, O. R.: Proc. AGARD Symp. on Flow Separation, held in Göttingen, Germany, AGARD-CP-168, 1975.

11. Chapman, D. R., Kuehn, D., and Larsen, H.: NACA Rep. 1356, 1958.

12. Nielsen, J., Lynes, L., and Goodwin, F.: USAF FDL TR-65-107, 1965.

13. Werle, M. J., and Vatsa, V. N.: AIAA J., Vol. 12, 1974, pp. 1491-1497.

14. Lewis, J. E., Kubota, T., and Lees, L.: AIAA J. Vol. 6, 1968, pp. 7-14.

15. Carter, J. E.: NASA TR-R-385, 1972.

16. Jobe, C. E., and Burggraf, O. R.: Proc. Roy. Soc. A, Vol. 340, 1974, pp. 91-111.

17. Veldman, A.E.P., and van de Vooren, A. I.: Proc. 4th Int. Conf. on Numerical Methods in Fluid Dynamics, Lecture Notes in Physics, Vol. 35, Springer-Verlag, 1975, p. 423.

18. Melnik, R. E., and Chow, R.: NASA SP-347, 1975.

19. Daniels, P. G.: Quart, J. Mech. Appl. Math., Vol. 27, pt. 2, May 1974, pp. 175-191.

20. Sato, H., and Kuriki, K.: J. Fluid Mech., Vol. 11, pt. 3, 1961, pp. 321-352.

21. Daniels, P. G.: J. Fluid Mech., Vol. 63, pt. 4, 1974, pp. 641-656.

22. Chow, R., and Melnik, R. E.: Proc. 5th Int. Conf. on Numerical Methods in Fluid Dynamics, Lecture Notes in Physics, Springer-Verlag, 1977.

23. Brown, S. N., and Daniels, P. G.: J. Fluid Mech., Vol. 67, pt. 4, 1975, pp. 743-761.

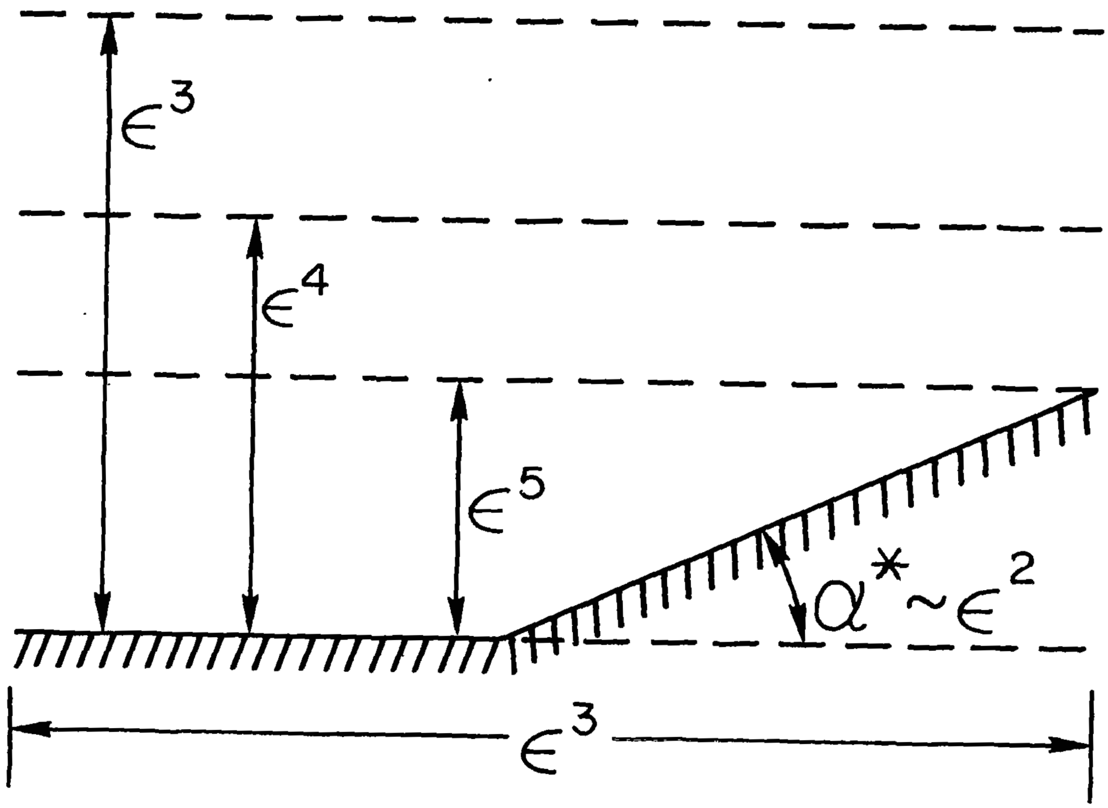

Figure 1.- Schematic of triple deck.

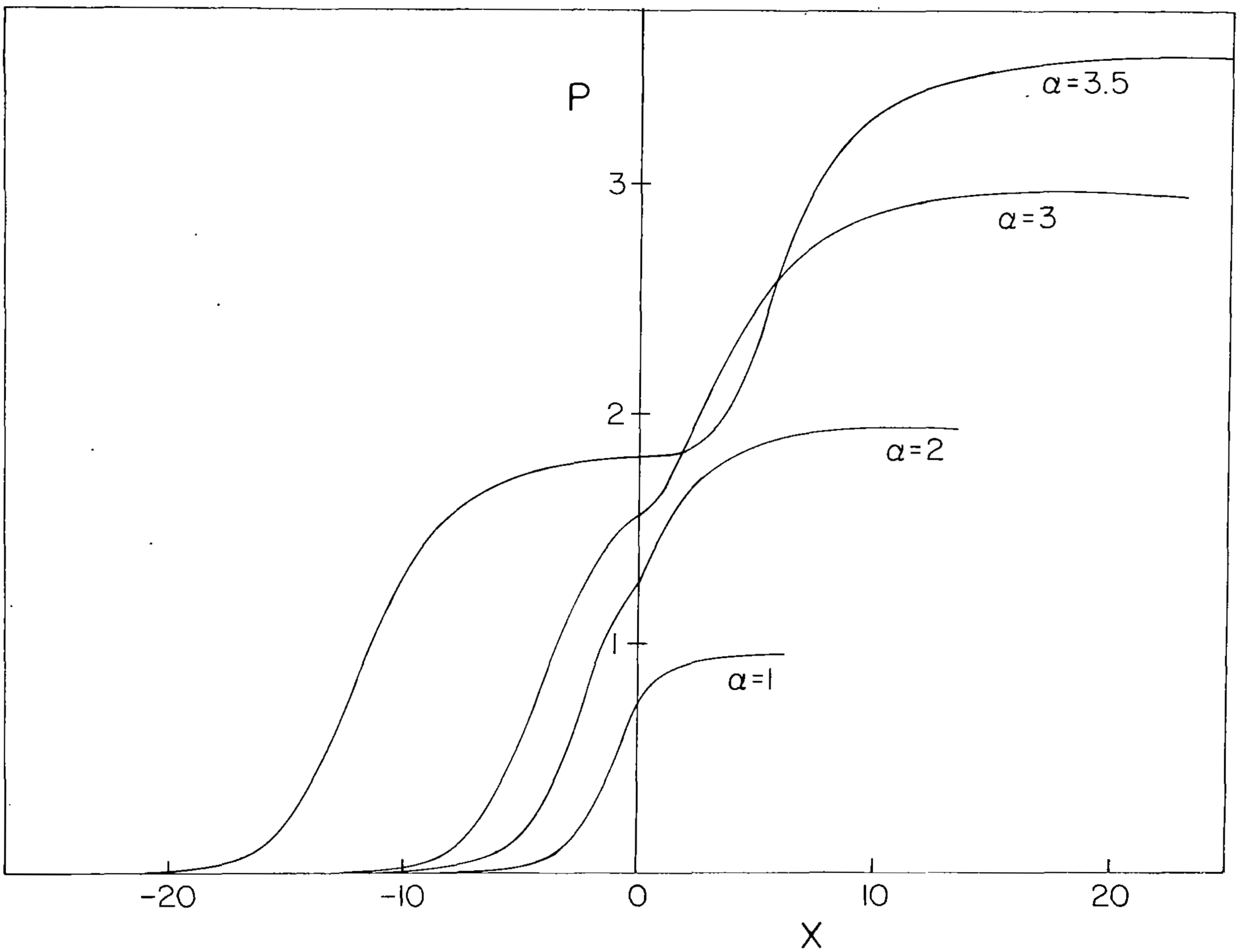

Figure 2.- Compression-ramp pressure distribution.

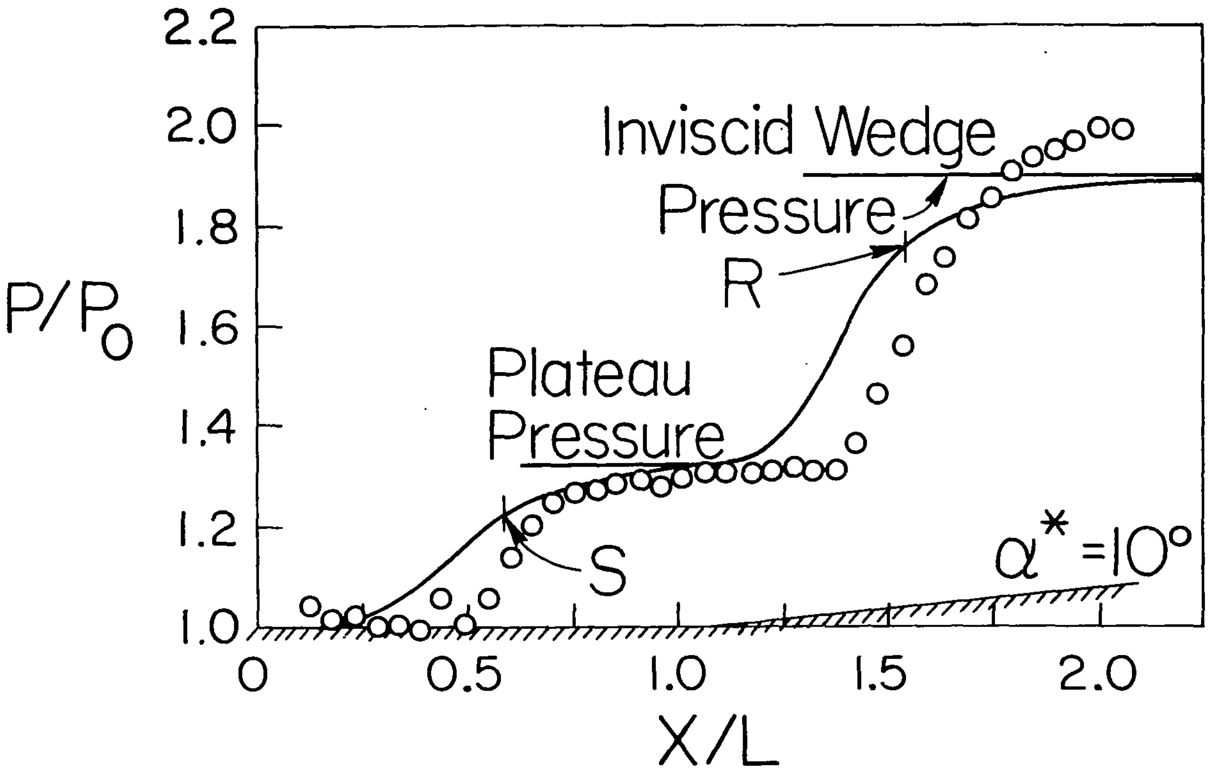

Figure 3.- Comparison of large α theory with experiment.

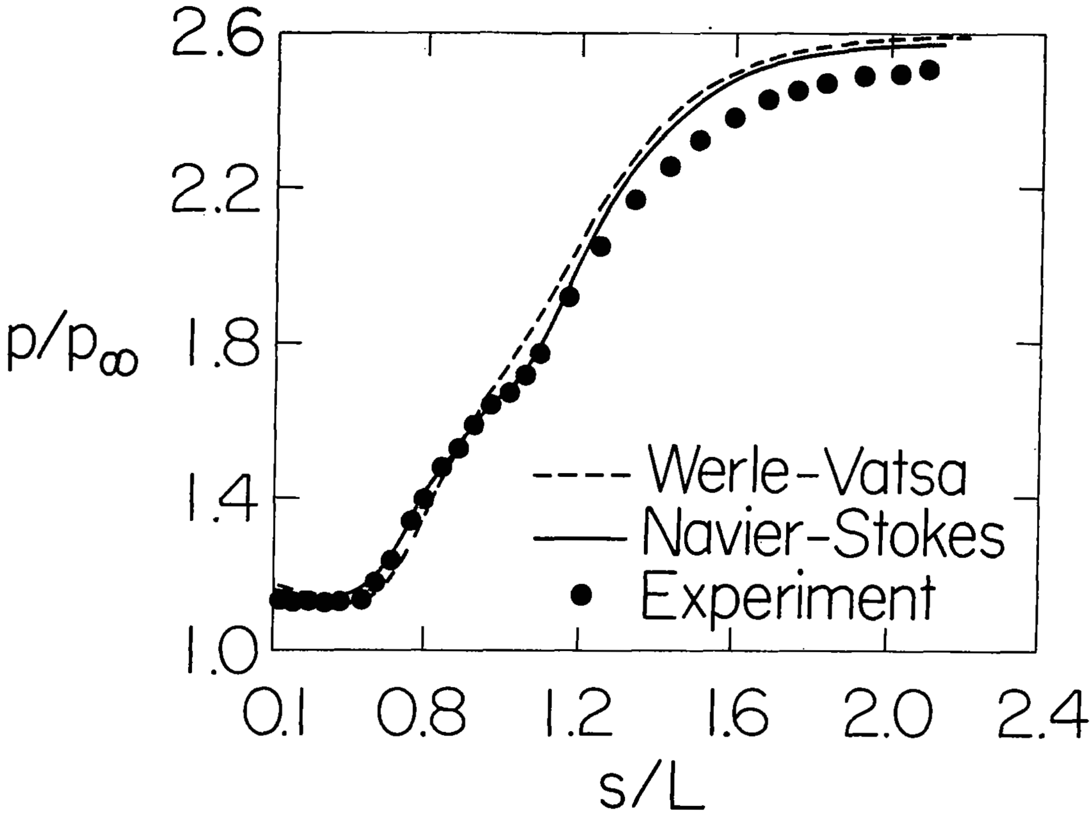

Figure 4.- Verification of interacting boundary layer model.

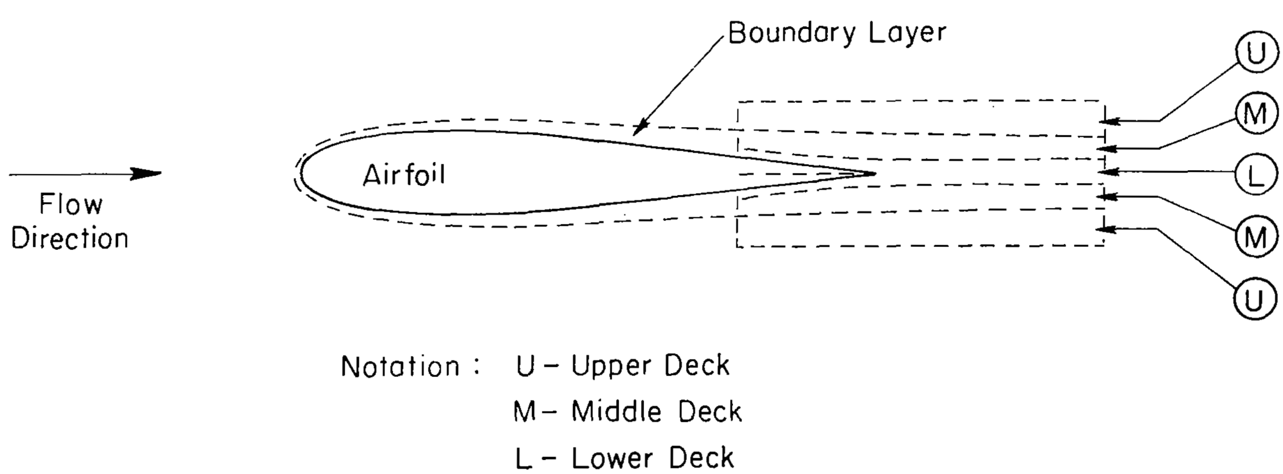

Figure 5.- Triple deck at trailing edge of airfoil.

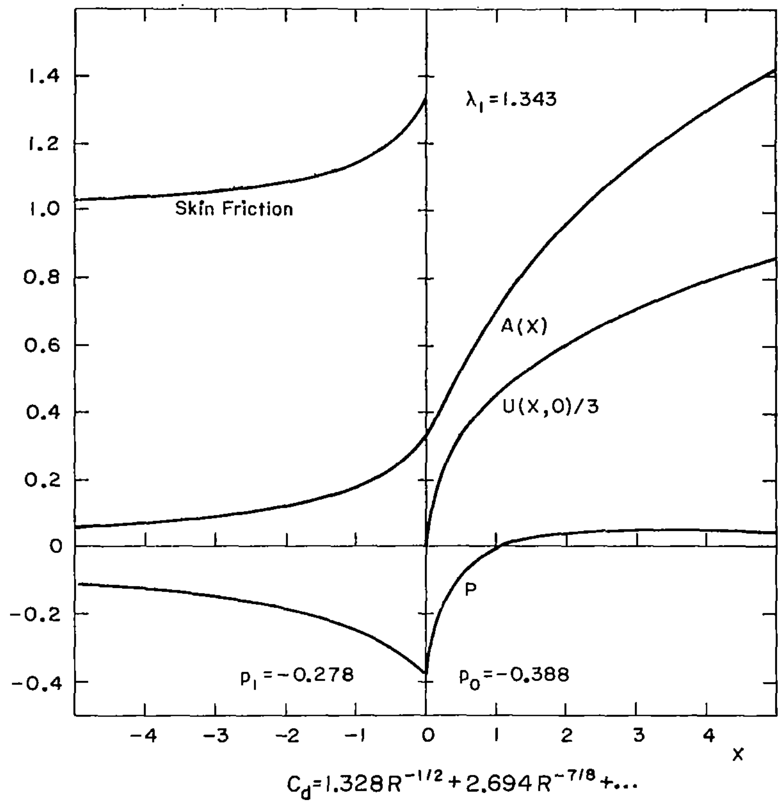

Figure 6.- Summary of trailing edge results.

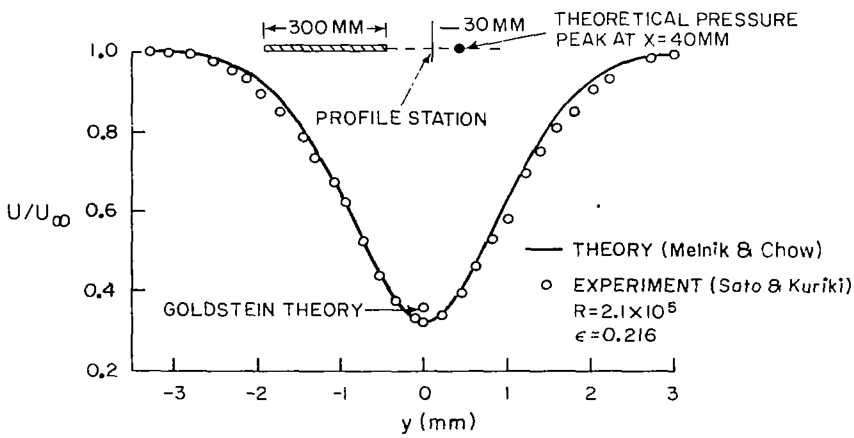

Figure 7.- Wake-velocity profile: theory vs. experiment.

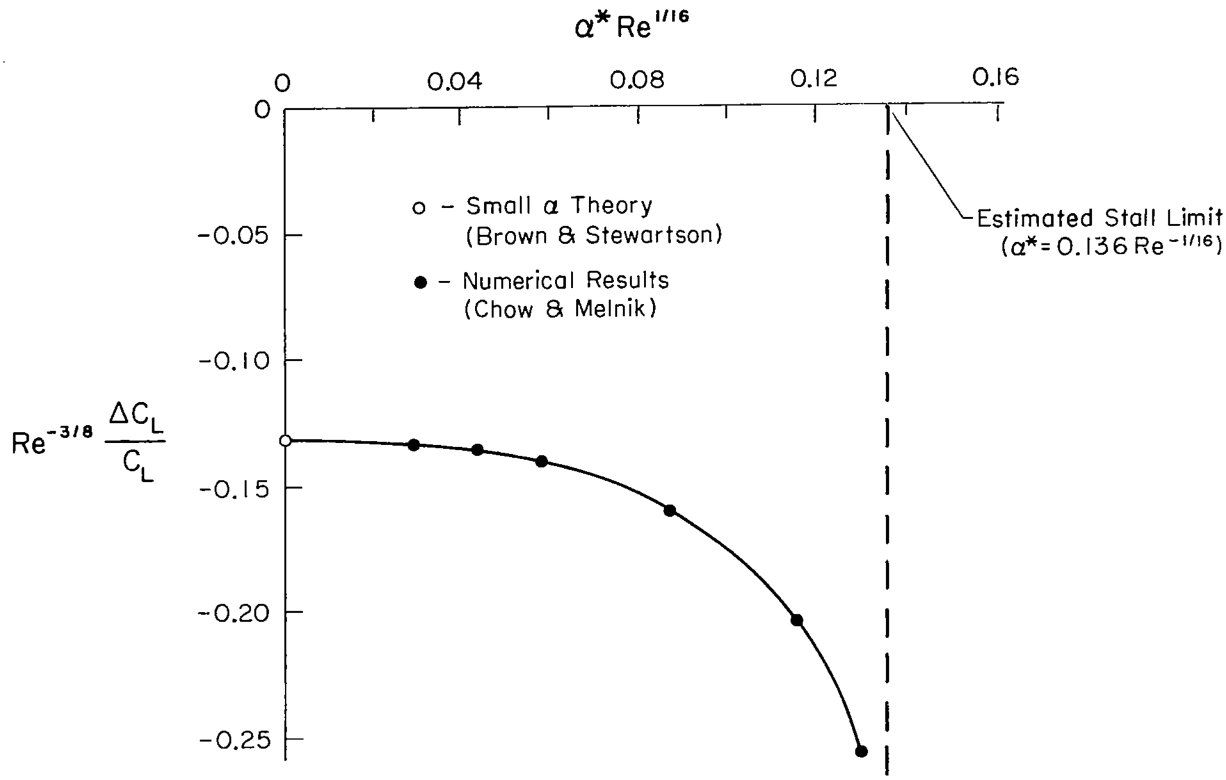

Figure 8.- Viscous correction to kutta condition for laminar flow.

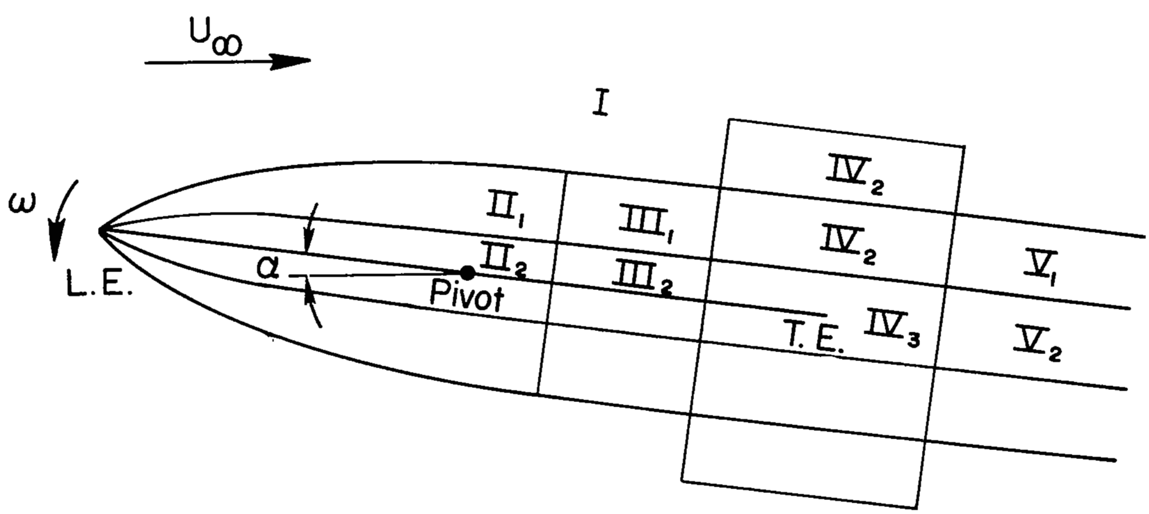

Figure 9.- Limit flow structure for oscillating plate.